Measurement of emission diameter as a function of time on foam z-pinch plasmas

S. E. Lazier, T. L. Barber

Ktech Corporation, 901 Pennsylvania Avenue NE, Albuquerque, New Mexico 87110

M. S. Derzon, J. W. Kellogg

Sandia National Laboratories, P.O. Box 5800 Albuquerque, New Mexico 87185

(Presented on 14 May 1996)

We have developed a streaked imaging capability to make time-resolved measurements of the emission size for low density foam z-pinches. By lens coupling visible emission from the z-pinch target to an array of fiber optics we obtained the emission profile in the visible as a function of time with radial resolution of 300 μm. To measure the emission at temperatures greater than ≈ 40 eV the source was slit-imaged or pin-hole imaged onto an x-ray filtered scintillator. Non-uniformity's in both visible and x-ray emissions were observed. We describe the diagnostics, the image unfold

DISCLAIMER

process, and results from the instrument for both visible and x-ray measurements.

I. INTRODUCTION

For this experiment the SATURN accelerator generated the current used to drive a low density foam z-pinch target.[1] To study the current initiation in the targets we developed a streaked imaging system capable of measuring emissions in the visible and x-ray.

The diagnostic recording system was fielded to make time-resolved measurements of emission size and uniformity for the low density foam z-pinch targets. Required design criteria for the diagnostic included; system bandwidth less than 2 ns, and a radial spatial resolution less than 300 μm. These were obtained by modifying an instrument used on PBFA II.[2]

II. DIAGNOSTIC HARDWARE

For this experiment two versions of the diagnostic were fielded. One instrument imaged the emissions from the targets on-axis, viewing from

the bottom; the second instrument was installed to image emissions from the side of the targets 32° up from the horizontal plane.

In the initial configuration for the on-axis diagnostic, visible emissions from the low density foam target were lens coupled onto an array of optical fibers. The fiber-optic array contained three fiber rows separated by 4.125 mm. The first two fiber rows contained 33 fibers 250 μm apart, the third fiber row had 24 fibers 125 μm apart. The lens used to image the target had a magnification of 1.25 giving a spatial sampling at the foam target of 200, 200, and 100 μm respectively for the three fiber rows. The other end of the fiber-optic array, containing 90 fibers 250 μm apart, was pulled into a screen room and proximity coupled to a streak camera with a sampling rate of .18 ns/pixel. The resulting image from the streak camera was lens coupled onto a 1024 x 1024 pixel CCD. The digitized image from the CCD was acquired with a Macintosh computer and processed with IPLab Spectrum image-processing software.

The series at SATURN consisted of 15 shots and three configurations of the diagnostics were used. To measure emission temperatures $\approx$ 20 eV the lens system described above was used. To measure emission temperatures $>$ 40 eV the low density foam was slit-imaged or pin-hole imaged onto an x-

ray filtered scintillator coated on a fiber-optic faceplate and proximity coupled to the input end of the fiber-optic array.

III. IMAGE PROCESSING

Several steps were taken to measure and compensate for various environmental, hardware induced, or shot induced effects present in the data. Fig. 1 shows a portion of a digitized streak camera image before image processing. Time is represented by the x-axis, fiber number (and therefore position) by the y-axis, and signal amplitude is represented by intensity. This portion of the streak camera image shows data from the middle row of fibers in the fiber-optic array. In the configuration used to obtain this image this series of fibers collected light generated by x-rays slit imaged onto an aluminum and scintillator coated faceplate. The diagnostic was aligned along the z-pinch axis viewing the bottom of the target.

The first step in processing the image was to subtract the background signal. Background images, images taken with no data present, measure the amount of signal generated by sources including; streak camera output with zero input, CCD background levels, and room light "leaking" into the system. Background signals were obtained immediately after each data field

was collected while the diagnostic was still in shot configuration. The background images were then subtracted from the data images.

The second image processing step was to compensate for random noise by performing a 3 by 3 pixel blur on the data image followed by a 3 by 3 pixel enhancement. The 3 by 3 pixel blur was done by summing the pixel amplitude with the surrounding 8 pixel amplitudes and dividing by 9. The pixel 3 by 3 pixel enhancement multiplied the pixel amplitude by 9 and subtracted the surrounding 8 pixel amplitudes.

For the third step the image was segmented, measured, and stored in a data table To segment the data an overlay was created defining regions of the image to be analyzed. To create the overlay a minimum pixel value (just above background) was chosen, all pixels with values greater than the minimum are included in the overlay; segments are defined as groups of adjoining pixels meeting the overlay criteria. The overlay used to analyze the data image divided each fiber output into one segment. Each segment was then split into regions three pixels wide, effectively dividing the light from each fiber into 0.54 ns sections. The amplitude of light for each pixel in the 0.54 ns wide section was summed and stored as an entry in a table. This procedure was performed for every 0.54 ns section in each of the fibers, generating a column of data.

To correct for non-uniformity's in the CCD imaging array, non-uniform attenuations of the individual fibers in the fiber-optic array, and non-uniform coupling at the streak camera input a flat field correction was performed as the fourth image processing step. Flat fields, images of a uniform light source, measure the relative attenuations of the components in the diagnostic. Flat field images, obtained by recording the output of a flashlamp-driven integrating sphere with the diagnostic in shot configuration, were taken periodically throughout the shot series to ensure similar system configuration for flat field data and shot data.

First, the flat field images were processed similarly to the data images using background subtraction, blur/enhance, and segmentation techniques. The flat field images were then processed using the same segmentation overlay as the data image to ensure identical image sections were analyzed. Data from the flat field was stored in a separate column of the data table. Since the effects of non-uniformity's are multiplicative by nature the column of shot data was then divided by the column of flat field data leaving a column of flat field corrected data.

The final step of the image processing was to correct for the effects of the bremsstrahlung radiation pickup in the fibers. To measure bremsstrahlung radiation effects on the detected signal, light from a HeNe

laser was sent down a fiber in the fiber-optic array, looped through the diagnostic end of the fiber-optic array, sent back up the fiber-optic array, and recorded as one of the streaks on the streak tube along with the shot data. Since the HeNe output is constant (for the 200 ns streak camera sweep) and the fiber loop was not exposed to direct emissions from the low density foam target, any amplitude change, positive or negative, observed on the streak camera trace representing the HeNe laser was due to bremsstrahlung radiation effects on the fiber loop.

To correct for bremsstrahlung radiation pickup, the flat field corrected data column was first mapped onto a two dimensional table; each row representing a different fiber, each column representing a different 0.54 ns amount of time. Data from the HeNe laser was processed with the shot data using the techniques described above and consequently mapped into one row of the table. This row represented the amplitude of the HeNe laser plus the amplitude of the bremsstrahlung radiation. Then, the signal amplitude of the HeNe (measured before bremsstrahlung radiation effects) was subtracted from the data row leaving a row of data containing only the effects of the bremsstrahlung radiation. This data row was subtracted from the rows containing shot data, removing the bremsstrahlung radiation effects and completing the image processing procedure.

The resulting table, viewed as a 3-D chart, with signal amplitude represented by arbitrary gray scaling in the z-axis is shown in Fig. 2. Time and fiber position numbers for Fig. 2 are accurate at the target but relative and have not been calibrated back to the shot time line or the target geometry as yet. It should also be noted that, due to the slit configuration used for this shot, the light entering each fiber represents the sum of light for a rectangular region of the target. The size of the region is defined by the core size of the fiber, the size of the slit, and the position of the slit between the fiber-optic array and the target. Each fiber in Fig. 2 collected light from a region ≈ 1.5 cm x 170 μm, region centers were 200 μm apart. The y-axis for Fig. 2 represents the position of the region being sampled, data from the chart is a measure of the total emissions for any given region at any given time.

IV. SYSTEM CALIBRATIONS AND PROPERTIES

To provide a time reference on the streak tube image, four fibers were added to the streak camera end of the fiber-optic array in addition to the 90 data fibers. Signals from these fibers were recorded along with the shot data. Two fibers transmitted a time-referenced impulse signal to correlate

the data to the other diagnostics on the shot series, and two fibers transmitted a comb signal, generating a light pulse every four ns, to provide a time base for the streak camera image.

A criteria was developed to determine when the system saturated due to effects such as signal amplitude, and photocathode intensity distribution and current saturation in the streak camera. Defining resolution as IMax / IMin, where IMax is the amplitude of the data signal and IMin is the amount of signal present between data streaks we identified saturation as occurring at the amplitude at which the resolution starts to fall. We plotted resolution versus IMax the results are shown in Fig. 3. This figure shows data from the same fiber on two shots where saturation was detected. On shot 2263 the entire photocathode was illuminated due to bremsstrahlung radiation pickup and the resolution starts to fall off at an IMax of 2000 counts. On shot 2258 the signal amplitude for two fibers got to large saturating a small portion of the photocathode and resolution doesn't fall off until IMax gets to 7500 counts. The resolution criteria was used to determine which data was meaningful and at what point the signal strength exceeded system capabilities. Raw CCD noise was 2 counts giving a worst case dynamic range to noise ratio of 2000/2 or 1000 to 1.

V. RESULTS

Early in the shot series the diagnostic was lens coupled to the low density foam target to determine if the initial current sheath surrounding the target was uniform or filamented. In this most sensitive configuration low levels of light could be detected which gives a good idea of initial current-sheath structure. Fig. 4 shows a processed image of the solid aerogel target[3] for shot 2257 viewed off-axis. The off-axis diagnostic was identical to the on-axis diagnostic described above with two exceptions; the radial resolution of this diagnostic was 500 μm at the target (a feature of the fiber array used), and the diagnostic viewed the side of the target angled 32° to the horizontal plane. In the lens coupled configuration each fiber represents a section of one horizontal slice of the target. The sections for this configuration were round with 80 μm diameters and 500 μm centers. The data in Fig. 4 corresponds to the total light at a particular section of the horizontal slice at any given time. The visible light recorded is limited to the 400-800 nm range by the bandpass constraints of the fiber bundle, lens, and streak camera sensitivity. The x-axis times are accurate relitivistically but have not been calibrated absolutely back to the shot time line as yet.

The data shows different sections getting hot at different times, the fiber positioned at 4.5 mm sees emissions starting at 34 ns while fiber position 2.5 sees peak emissions at 80 ns.

Non-uniform emissions were also detected using a pin-hole imaged x-ray configuration on shot 2258, the target was a solid aerogel foam with 1200 Å Au coating[1] (Fig. 5). With the pin-hole configuration each fiber viewed emissions from an ≈ 1.8 mm diameter circular region of the target, region centers were 500 μm apart on a horizontal line across the side of the target. As with the visible data, the x-ray data shows different spots getting hot at different times. The fiber positioned at 2 mm detects high emissions at 20 ns while the fiber positioned at 5 mm sees peak emissions at 85 ns, 65 ns later. However, the fiber positioned at -2 mm sees relatively low emissions throughout the implosion. This clearly indicates a non-uniform current amplitude with respect to time, indicating these foam targets experienced filamentation in the current sheath during the z-pinch.

The on-axis diagnostic measured x-ray emission spot sizes at three energy cuts for each shot late in the shot series. The targets for these shots were 4 mm diameter, 5mg/cc aerogel foams placed inside a tungsten wire array[3] and viewed through 6.5 mm diameter hole. Aluminum filtered x-rays (≈50-80 eV) are shown in Fig. 2. Similar images for titanium filtered x-rays

(400-450 eV) and carbon filtered x-rays (200-280 eV) were also obtained. Calculating emission spot radius from the FWHM and plotting vs. time for the titanium cut gives the plot in Fig. 6.

Emission spot implosion velocities were estimated by measuring the slope of the tangent to a second degree polynomial curve fit applied to the emission spot radius vs. time curve in Fig. 6. Uncertainties are estimated at plus or minus 6 percent.

The emission spot implosion velocity calculated for the titanium energy cut in Fig. 6 is 12 cm / μsec. Calculations for the other energy cuts give emission spot implosion velocities of 34 cm / μsec (carbon) and 104 cm / μsec (aluminum). For this shot the calculated z-pinch implosion velocity was 30 cm / μsec indicating that the diagnostic will not be a useful tool for measuring z-pinch velocities until more work is done to correlate x-ray emissions to mass implosions in the foam targets.

VI. SUMMARY

A diagnostic obtaining a continuous time-resolved measurement of emissions from low-density foam targets has been fielded on the SATURN accelerator. Criteria for determining camera saturation were described and

used to determine when signal amplitudes from the target or bremsstrahlung radiation pickup exceeded the linear gain of the diagnostic. The image processing methodology provided images that show non-uniform emission in both visible and x-ray from all the low density foam targets. The measured x-ray emissions were not a good indicator of z-pinch implosion velocities in wire array targets.

ACKOWLEDGMENTS

This work would not have been possible without the support and efforts of Blake Henderson and the rest of the SATURN support crew. We would also like to thank Mike Hurst for his help fielding the diagnostic. This work is supported by the U.S. Department of Energy under Contract DE-AC04 #94AL85000.

[1] M. S. Derzon *et.al.*, these proceedings.

[2] M. S. Derzon *et. al.*, SPIE Vol. 2002, 31 (1993).

[3] C. Deeney, *et. al.*, these proceedings.

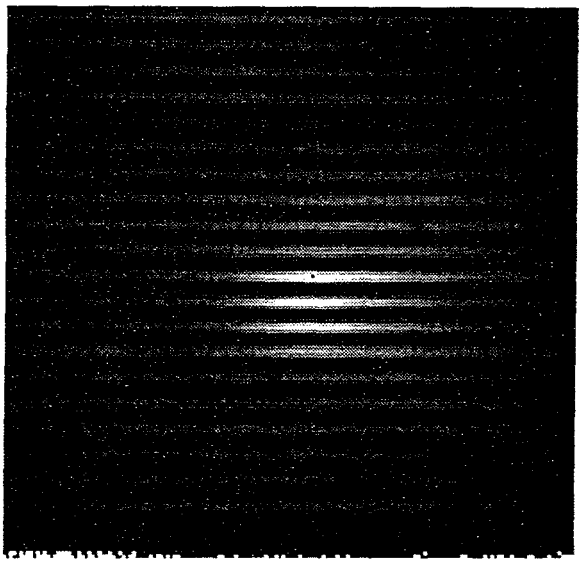

FIG. 1. Portion of unprocessed streak camera data for shot 2262 with time in the x-axis, fiber position in the y-axis, and signal amplitude represented by intensity.

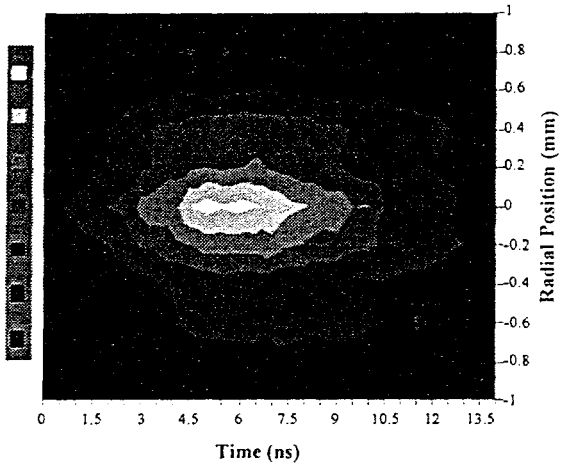

Fig. 2. Processed streak camera data showing radial position vs. time, signal amplitude is shown by gray scaling.

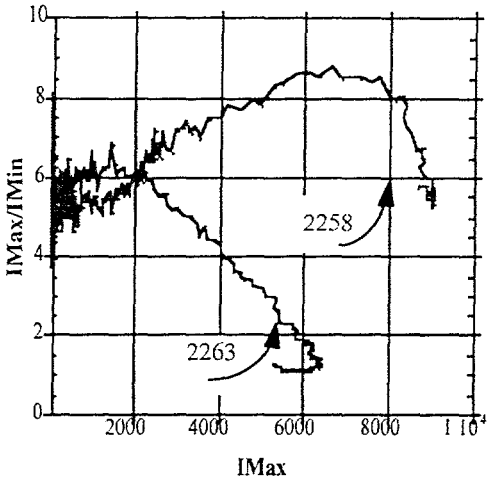

Fig. 3. Resolution (IMax/IMin) vs. IMax for same fiber on different shots. Saturation occurs when resolution starts to fall off.

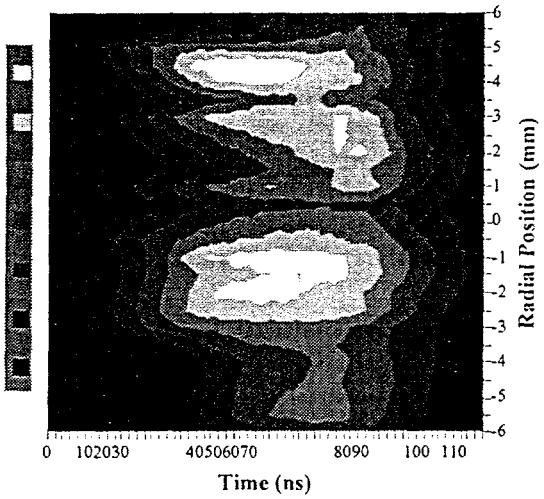

Fig. 4. Visible light image of shot 2257 shows radial position on the target vs. time, gray scaled signal amplitudes indicate target areas heating at different times.

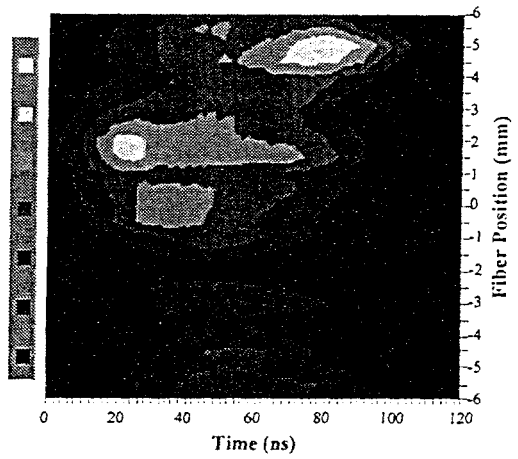

Fig. 5. X-ray image of shot 2258 showing radial position at the target vs. time, z-axis amplitude gray scaling indicates filamentation in current sheath.

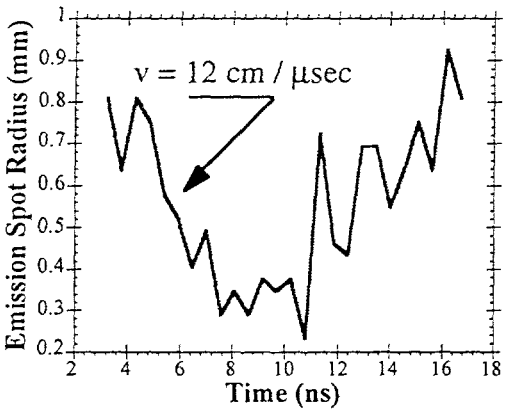

Fig. 6. Emission spot size vs. time for titanium filtered x-rays (400-450 eV) on shot 2262. Calculated emission spot implosion velocity is 12 cm/μsec.